ITTC Quality System Manual

Recommended Procedures and Guidelines

Procedure

Uncertainty Analysis - Example for Waterjet Propulsion Test

7.5	Process Control
7.5-02	Testing and Extrapolation Methods
7.5-02-05	High Speed Marine Vehicles.
7.5-02-05-03.3	Uncertainty Analysis - Example for Waterjet Propulsion Test

Updated / Edited by	Approved
Propulsion Committee of the 28th ITTC	28th ITTC 2017
Date 06/2017	Date 9/2017

Table of Contents

Uncertainty Analysis - Example for Waterjet Propulsion Test

1. PURPOSE OF PROCEDURE

The purpose of the procedure is to provide an example for the uncertainty analysis of a model propulsion test with waterjets, following the ITTC procedures 7.5-02-01-01 Rev 00, “Uncertainty Analysis in EFD, Uncertainty Assessment Methodology” and 7.5-02-01-02 Rev 01, “Uncertainty Analysis in EFD, Guidelines for Towing Tank Tests”.

2. PARAMETERS

2.1 Nomenclature

The nomenclature that is specific to this example of uncertainty analysis is given here.

A_N	Nozzle discharge area
c_{es}	Energy velocity coefficient
c_{ms}	Momentum velocity coefficient at station *s*
E_s	Total energy flux at station s (kinetic + potential + pressure)
$E_{s\xi}$	Total axial (in ξ-direction) energy flux at station s
D_N	Nozzle discharge diameter
F_D	Skin friction correction in a self-propulsion test carried out at the ship self-propulsion point
H_{JS}	Jet System Head
K_Q	Impeller torque coefficient
K_{QJ}	Flow rate coefficient
$\overline{M}_{is}$	Momentum flux at station *s* in *i* direction
NVR	Nozzle velocity ratio: $NVR = \frac{\overline{u}_{6\xi}}{V_0}$
n	Impeller rotation rate
P_D	Delivered power to pump impeller
P_{JSE}	Effective Jet System Power: $P_{JSE} = Q_J H_{JS}$
Q	Impeller torque
Q_J	Volume flow rate through waterjet system
T_{Jx}	Jet thrust (can be measured directly in bollard pull condition)
t	Thrust deduction fraction: $(1-t) = \frac{R_{TBH}}{T_{net}}$
U_0	Free stream velocity
u_{is}	velocity component in i-direction at station *s*
$\Delta\overline{M}_x$	Change in Momentum Flux in x-direction
Δp	Pressure differential of flow rate transducer
w_1	Geometric width of intake at station 1
w_{1A}	Maximum width of capture area
z_6	Vertical distance of nozzle centre relative to undisturbed surface
η_{eI}	Energy interaction efficiency: $\eta_{eI} = \frac{P_{JSE0}}{P_{JSE}}$
η_I	Ideal efficiency, equivalent to jet efficiency in free stream conditions
η_{INT}	Total interaction efficiency
η_{JS}	Jet System efficiency
η_{mI}	Momentum interaction efficiency: $\eta_{mI} = \frac{T_{net0}}{T_{net}}$
η_0	Free stream efficiency: $\eta_0 = \eta_P\, \eta_{duct}\, \eta_I$
θ_N	Jet angle relative to the horizontal at the nozzle (station 6).

Subscript $_0$ indicates free stream conditions

3. EXAMPLE FOR WATERJET PROPULSION TEST

This procedure provides an example showing an uncertainty assessment for the results from a model propulsion test with waterjets. The bias and precision limits and total uncertainties for single and multiple runs have been estimated for the flow rate Q_J, the change in momentum flux $\Delta\overline{M}_x$ and effective jet system power P_{JSE}.

A further uncertainty analysis on delivered power P_D and the total interaction effect including the thrust deduction factor $(1-t)$, has not been worked out here. These uncertainties can be determined after an uncertainty analysis of the waterjet system tests and the bare hull resistance test has been conducted (see Fig. 1).

Furthermore, extrapolation to full scale has not been considered in this example. Although it might lead to significant sources of error and uncertainty, it is not essential for the present purpose of demonstrating the methodology.

When performing an uncertainty analysis for a real case, the details need to be adapted according to the equipment used and procedures followed in each respective facility.

3.1 Test Design

There are essentially two roads that lead to a prediction of the power-speed relation $P_D(U_0)$.

The shortest road leads via the measured effective jet system power P_{JSE} from the propulsion test and the internal jet system efficiency η_{JS} from the waterjet system tests:

$$P_D = \frac{P_{JSE}}{\eta_{JS}} \quad (1)$$

The second road gives a more complete review of all powering parameters. It includes apart from the delivered power P_D-prediction also a full prediction of all jet-hull interaction terms. The power prediction is then based on a prediction of the resistance or effective power P_E and the overall efficiency η_D. The delivered power can thus be obtained from:

$$P_D = \frac{P_E}{\eta_D} \quad (2)$$

The first route should theoretically lead to the smallest uncertainty, as the additional uncertainty of the bare hull resistance is not included in the power prediction, whereas it does enter in the uncertainty for the second route (through the thrust deduction fraction t).

3.2 Measurement Systems and Procedure

Figure 1 shows a block diagram for the waterjet propulsion test, including the individual measurement systems, measurement of individual variables, data reduction and experimental results.

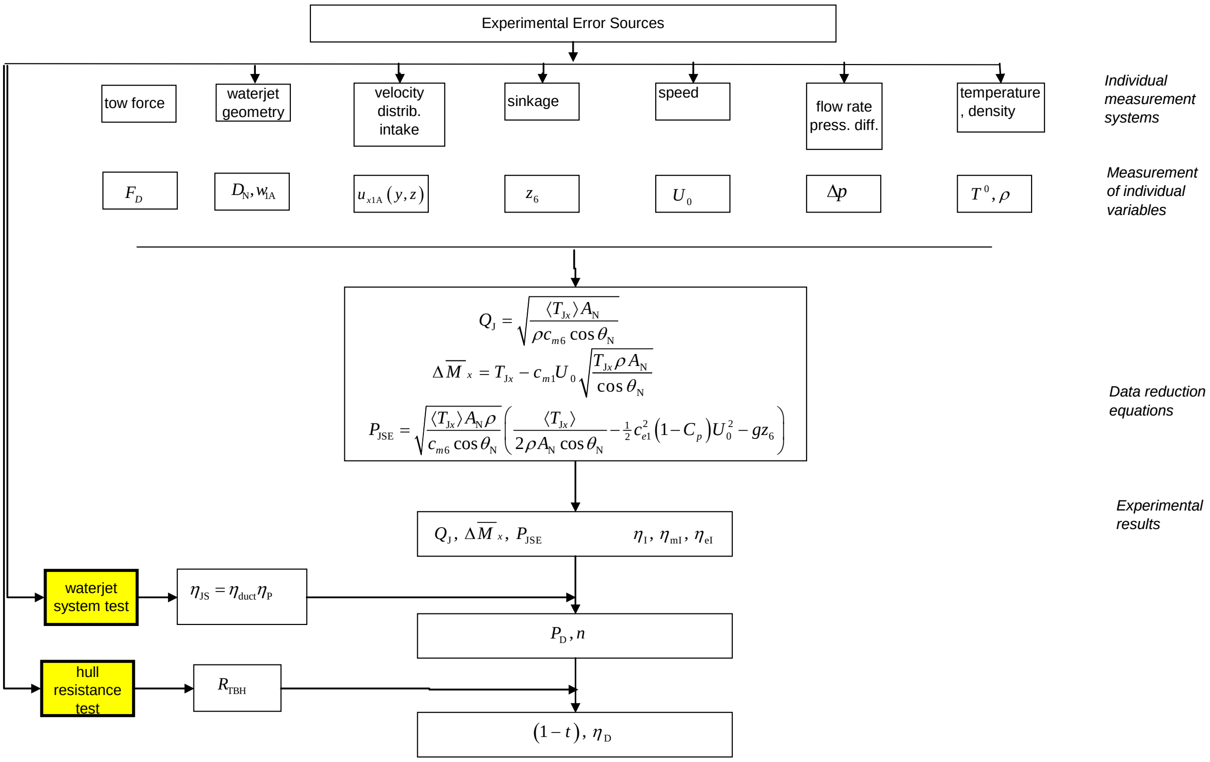

Figure 1 Block diagram for the waterjet propulsion test.

To enhance the process of identifying and estimating the elementary bias limits for each measurement system, four categories of error sources are distinguished:

- calibration
- data acquisition
- data reduction
- conceptual bias

The bias limits of the input parameters are subsequently reduced into the bias limits for the results by using the data reduction equations of Figure 1.

The precision limits for model scale are estimated by an end-to-end method for multiple tests (M) and a single run (S).

The $\pm U_i$ uncertainty interval about the measured value of X_i is the band within which the experimenter is 95 per cent confident the true value of the variable lies. The 95% confidence uncertainty is given by:

$$U_i = \sqrt{B_i^2 + P_i^2} \tag{3}$$

Instead of using the dimensional sensitivity, it is often more convenient to use a non-dimensional sensitivity θ'_i, relating the non-dimensional error in the result b'_R to the non-dimensional error in the source parameter b'_i:

$$b'_R = \sqrt{\sum_{i=1}^{k} (\theta'_i b'_i)^2} \tag{4}$$

where the non-dimensional bias error is defined by:

$$b'_i = \frac{s_i}{X_i} \quad (5)$$

and the non-dimensional sensitivity by:

$$\theta'_i = \frac{\partial R}{\partial X_i}\frac{\overline{X}_i}{\overline{R}} \quad (6)$$

A similar result is found for the non-dimensional precision error p'_i. The advantage of normalizing the error contributions in this fashion is that all error contributions and sensitivities can be compared immediately for their relevance in the final result.

The elemental bias limits $(B_i)_k$ must be estimated for each variable X_i using the best information one has available at the time. Manufacturers' specifications, analytical estimates and previous experience have typically provided the basis for most of the estimates. Estimates for the bias errors here have been largely based on the results from the standardization tests.

Additional conceptual bias errors resulted from not measuring directly the variable in the data reduction equation. An example of such an error is the error that results from assuming that the vena contracta in the jet coincides with the nozzle discharge opening (station 6 instead of station 7 is used for the determination of momentum and energy fluxes).

The precision limit in the pressure difference over the transducer has been determined, from which the flow rate and momentum and energy fluxes are derived. This limit has been determined with an end to end method, where all the precision errors for speed, pressure transducers, impeller revolutions and temperature / density are included. Regardless as to whether the precision limit is to be determined for single or multiple runs, the standard deviation must be determined from multiple tests in order to include random errors. If it is not possible to perform repeated tests, the experimenter must estimate a value for the error using the best information available at that time. The error has then become a bias error.

The precision limit for multiple tests is calculated according to:

$$P(M) = \frac{K.S_{\mathrm{Dev}}}{\sqrt{M}} \quad (7)$$

where M = number of runs for which the precision limit is to be established, S_{Dev} is the sample standard deviation established by multiple runs and the so called coverage factor K depends on the distribution of the error. For a Gaussian distribution of the error and a large sample, this K factor equals approx. 2 (see also ITTC procedure 7.5-02-01-01 "Uncertainty assessment methodology").

The precision error for a single run can be calculated from:

$$P(S) = K.S_{\mathrm{Dev}} \quad (8)$$

3.3 Uncertainty Analysis

This section presents the results of the uncertainty analysis for jet thrust from the nozzle $T_{\mathrm{J}x}$, flow rate Q_{J}, change in momentum flux $\Delta\overline{M}_x$ (or net thrust) and effective jet system power P_{JSE}. The uncertainty analysis is conducted for the Athena at a speed of 25 kn. The results are valid for model scale. Extrapolation and conversion of effective jet system power to delivered power to the pump impeller are not included here.

In Table 1 and Table 2, the principal particulars of the model and the constants used in the example are presented.

Table 1 Athena model particulars

Definitions	**Symbol**	**Value (unit)**
Length model	L_{PP}	5.486 m
Displacement Vol model	∇	0.4218 m^3
No. of waterjets		2
Nozzle diameter	D_N	0.0846 m
Waterjet intake width	w_1	0.125 m

Table 2 Constants for Athena model tests

Definitions	**Symbol**	**Value (unit)**
Gravity	g	9.81 m/s^2
Density, model basin	ρ	1000 kg/m^3
Kinematic viscosity	ν	1.139 10^{-6} m^2/s
Water temperature (test average)	T^0	15.0 deg

3.3.1 Jet thrust from nozzle

Table 3 presents the uncertainty results for the best estimate of the jet thrust $\langle T_{Jx} \rangle$as determined from the propulsion tests. As this thrust cannot be measured directly, it is determined from a Differential Pressure transducer that is calibrated during a bollard pull test. An important assumption that is made here is that the relation between jet thrust from the nozzle and pressure reading is the same during calibration in bollard pull condition and during the propulsion tests.

A conceptual bias error in the ratio $T_{jetx}/T_{jetx\,cal}$ is introduced to account for the uncertainty about the equality of this relation in both tests. The best estimate for the jet thrust is consequently given by:

$$\langle T_{Jx} \rangle = T_{Jxcal} \frac{T_{Jx}}{T_{Jxcal}} \tag{9}$$

where the calibrated jet thrust is obtained from:

$$T_{Jxcal} = a_0 + a_1 Dp \tag{10}$$

and a_i denotes the calibration coefficients.

Table 3 Uncertainty analysis jet thrust T_J prediction from propulsion test

Error source	Mean value	Non dimensional sensitivity	Precision error	Bias error	$(K\theta'_i s'_i)^2 + (\theta'_i b'_i)^2$	Comments
		θ_i'	s$_i$' [%]	b$_i$' [%]		
a_0	0.605	0.00	20		0.00	mean value from ITTC-tests, error estimate (Van Terwisga, 1996)
a_1	0.198	1.00	0.2		0.16	“
Δp	4.37E+04	1.00	0.04	1	1.01	“
T_{Jx}/T_{Jxcal}	1.00	1.00		1.1	1.21	error estimate (Van Terwisga, 1996)
Totals			0.20	1.49		
			URSS@95%		1.54	

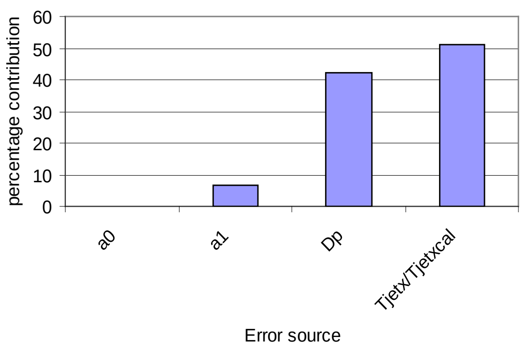

Figure 2 Relative importance of errors in jet thrust over sources.

Figure 2 shows that the differential pressure transducer and the error in the assumption that the jet thrust calibration during bollard pull can be used during propulsion tests are the dominant error sources. The total uncertaintyURSS(TJx) in jet thrust is estimated to be approx. 1.5% for the Athena at a speed of 25 kn.

With the uncertainty in $\langle T_{Jx} \rangle$, the uncertainty in flow rate, thrust and power can subsequently be determined.

3.3.2 Flow Rate.

Applying the bollard pull thrust for calibration of the flow rate, this flow rate is given by:

$$Q_J = \sqrt{\frac{\langle T_{Jx} \rangle A_N}{\rho c_{m6} \cos\theta_N}} \quad (11)$$

Table 4 presents the uncertainty analysis for the flow rate.

Table 4 Uncertainty analysis flow rate prediction

Error source	Mean value	Non dimensional sensitivity	Precision error	Bias error		Comments
		θ_i'	s_i' [%]	b_i' [%]		
T_{Jx}		0.50	0.20	1.49	0.594	From Table 3
A_N		0.50		0.8	0.160	
P		-0.50	0.0182		0.000	
c_{m6}	0.98	-0.50		2	1.000	
θ_N	3	0.00		5	0.000	
Totals			0.10	1.31		
			URSS@95%		1.32	

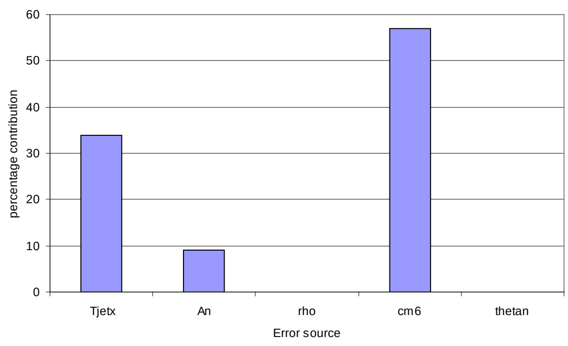

Figure 3 Relative importance of errors in flow rate over sources.

Figure 3 shows that the dominant error sources for the flow rate are the jet thrust and the momentum velocity coefficient for the velocity field at the nozzle discharge (station 6).

3.3.3 Change in Momentum Flux.

The change of momentum flux over the waterjet control volume is a best estimate for the net thrust T_{net}.

This change in momentum flux is obtained from:

$$\Delta\overline{M}_x = T_{\text{J}x} - c_{m1} U_0 \sqrt{\frac{T_{\text{J}x}\rho A_{\text{N}}}{\cos\theta_{\text{N}}}} \qquad (12)$$

The results of the uncertainty analysis are presented in Table 5. The distribution of errors over the distinct sources is presented in Figure 4. It is shown here that the dominant error sources are again in the jet thrust estimate and also in the momentum velocity coefficient in the capture area at Station 1A.

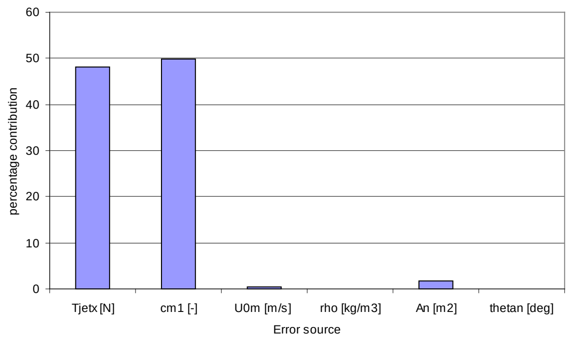

Figure 4 Relative importance of errors in change in momentum flux over sources.

Table 5 Uncertainty analysis of change of momentum flux prediction

Error source	Mean value	Non dimensional sensitivity	Precision error	Bias error		Comments
		θ_i'	s_i’ [%]	b_i’ [%]		
T_{Jx} [N]	313.00	1.55	0.20	1.49	5.731	From Table 3
c_{m1} [-]	0.89	-1.11	0.02	2.2	5.939	
U_0m [m/s]	4.40	-1.11	0.09	0.08	0.048	
ρ [kg/m^3]	1000.00	-0.55	1.82E-02		0.000	
A_N [m^2]	0.00562	-0.55		0.8	0.196	
θ_N [deg]	3.00	0.00		5	0.000	
NVR	1.70					
Totals			0.33	3.39		
			URSS@95%		3.45	

3.3.4 Effective Jet System Power.

The effective jet system power PJSE can be computed directly from the derived jet thrust, as given by eq. (13). The results of the uncertainty analysis for the effective jet system power PJSE are presented in Table 6. The distribution of errors over the distinct sources is presented in Figure 5. It is shown here that the dominant errors are caused by the jet thrust estimate and the nozzle area AN.

Table 6 Uncertainty analysis of effective jet system power P_{JSE}

Error source	Mean value	Non dimensional sensitivity	Precision error	Bias error		Comments
		q_i’	s_i’ [%]	b_i’ [%]		
T_{Jx} [N]	313.00	1.88	0.20	1.49	8.399	From Table 3
A_N [m^2]	0.00562	-2.71		0.8	4.700	
ρ [kg/m^3]	1000.00	1.00	1.82E-02		0.001	
c_{m6} [-]	0.98				0.000	
θ_N [°]	3.00			5	0.000	
c_{e1} [-]	0.89	-0.40	0.02	2.2	0.775	
U_0 [m/s]	4.40	-0.73	0.09	0.08	0.021	
g [m/s^2]	9.81	0.00			0.000	
z_6 [m]	0.07	0.01			0.000	
Totals			0.39	3.65		
			URSS@95%		3.62	

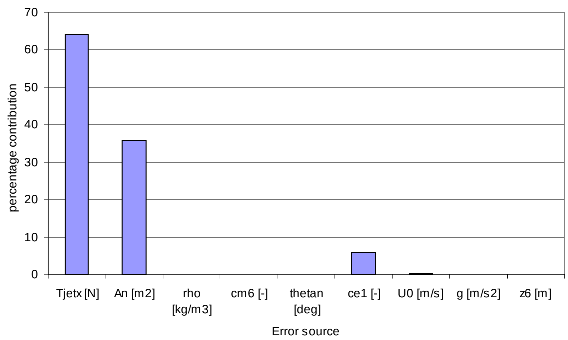

Figure 5 Relative importance of errors in effective jet system power.

$$P_{JSE} = \sqrt{\frac{T_{Jx} A_N \rho}{c_{m6} \cos\theta_N}} \left(\frac{T_{Jx}}{2\rho A_N \cos\theta_N} - \frac{1}{2} c_{e1}^2 \left(1 - C_p\right) U_0^2 - g z_6 \right) \quad (13)$$

4. REFERENCES

ITTC, 2005, "Report of Specialist Committee on Validation of Waterjet Test Procedures", ITTC Proc. of 24th ITTC.

Van Terwisga, T.J.C., 1996, "Waterjet-Hull Interaction", PhD Thesis, Delft University of Technology, April 1996, ISBN90-75757-01-8.